Environmental Health Perspectives
Vol. 9, pp. 81–94, 1974

Elemental Analysis of Asbestos Fibers by Means of Electron Probe Techniques

by Ivan B. Rubin* and Carl J. Maggiore†

The identification and characterization of microparticles has become an important field of study in recent years due to their presence in the environment and association with pathogenesis. Asbestos fibers have been intensively studied for these reasons. Since conventional microscopy has not provided unique identification of these materials, electron probe microanalysis, which yields chemical data, has been utilized in conjunction with other techniques to provide the necessary answers.

The options now available to undertake electron probe analysis are discussed with relation to their utilization for microparticle analyses. Two types of electron sources are available, thermionic and field emission. The x-ray spectroscopy requires the use of either wavelength-dispersive focussing crystal spectrometers or an energy-dispersive Si(Li) x-ray detector.

Data are presented to demonstrate the feasibility of asbestos identification by using modified raw data obtained with a scanning electron microscope and energy-dispersive x-ray spectrometer. Further, the extension of the technique to other microparticle identification problems is discussed.

Introduction

The relation of a variety of asbestiform minerals to disease is well documented *(1–3)*. Furthermore, the widespread use of these minerals has been demonstrated *(4)*. In order to monitor these health effects and the extent of environmental contamination by asbestos it is useful to be able to identify the different forms of the mineral rapidly, and with further progress to perform this identification routinely and eventually by automated techniques.

The problems are in large part separable when considered in terms of mineral types. The serpentine asbestos mineral, chrysotile, can be uniquely identified by its characteristic morphology when observed with the conventional transmission electron microscope *(5, 6)*. While it is relatively easy to recognize chrysotile visually, automating this procedure is of extraordinary complexity because it requires the solution of a variety of pattern recognition problems of great difficulty and is considered to be of questionable feasibility *(7)*.

Conventional transmission electron microscopy (TEM) and selected-area diffraction enable one to acquire sufficient morphological and structural information to identify a particle as a probable amphibole asbestos type. However, the structural and morphological differences between the amphibole asbestos minerals are not sufficient to enable one to identify the particle unambiguously.

It has been reported that amphiboles can be differentiated by the utilization of size distributions, but this technique is really applicable only to single fiber type populations or exposures *(8)*. Thus, it does not allow the characterization of individual fibers in a background of other particles from unknown sources which are usually the kinds of samples

*Environmental Sciences Laboratory, Mount Sinai School of Medicine of the City University of New York, New York 10029.

†Princeton Gamma Tech, Princeton, N.J. 08540.

environmental scientists, industrial hygienists, occupational physicians and pathologists are likely to encounter. Furthermore, as a matter of practicality, rapidity is an essential aspect of the technique, so that while there is recent evidence that careful application of selected area electron diffraction may allow separation of the amphiboles it would fail to meet the rapidity criterion. *(9)*.

If only the fact that some kind of amphibole were present was the only datum required, conventional TEM would be a suitable technique for the investigators previously mentioned. However, if automatic investigation of samples is required, the TEM method is even less applicable to the amphiboles than to chrysotile, because both morphology and diffraction data would be required and the automated operation of the microscope switching between selected-area diffraction and bright field modes would engender excessive complexities.

The chemistry of the minerals, along with size and shape (i.e., they are fibrous, $l/w > 3/1$) does allow further distinction when appropriate decision criteria are imposed. The quantitative accuracy of the chemical data need only be sufficient to allow identification, since that is the major interest. The use of electron microprobe analysis on a fiber-by-fiber basis is a technique which can be employed with success *(10,11)*. It has further application in the area of automated counting and sizing of fibers. If "identification only" chemical analysis is undertaken and fibers are an appropriate size (e.g., for chrysotile fibrils, 300–500 Å), a reasonably certain decision can be made by a computer operating on-line to count such a particle as a chrysotile fibril.

The Electron Microprobe Technique

The electron microprobe technique is based on the fact that a beam of high energy (5–40 kV) electrons incident on a target specimen generates x-rays characteristic of the elements present in that specimen. If the beam of electrons is suitably focussed, x-ray excitation is restricted to a relatively small volume (1 μm^3 or less), and chemical analysis of small volumes is possible. Therefore, there are two major components in a system designed to do microprobe analysis: the electron optical system to produce the focussed electron beam and associated imaging devices to allow the object under investigation to be observed and the x-ray spectrometry system which provides the means for determining the characteristics and quantity of x-rays generated in the object under analysis.

Electron Sources and Optics

In order to produce a focussed beam of high energy electrons, the electrons must be generated at the source, accelerated through the desired potential, and focussed by means of the optical system (lenses and apertures). There is now a choice of electron sources available, each having its own advantages. The first is the thermionic emitter (heated cathode) and the second is the field emitter (cold cathode) developed quite recently *(12, 13)*. The heated cathode is most useful where high currents in the focussed electron beam or probe are required and where spots of larger diameters are suitable. It is also the most useful when it is desirable to be able to vary currents over a wide range (10^{-6}–10^{-12} A). In this category, one can find the conventional tungsten hairpin filament and the more recently available higher brightness LaB_6 pointed filaments *(14)*.

The cold cathode source produces electrons by extracting them from a small (0.1–0.3 μm) tip of an oriented tungsten single crystal with an electrical field. Known as field emission, its higher brightness allows the production of higher current densities in spots smaller than 0.1 μm, e.g., at 250 Å spot diameter, heated tungsten provides 10^{-11} A, heated LaB_6 3×10^{-10} A, and field emission 10^{-9} A, $C_s \approx 20$ cm *(15)*. This is necessary to produce acceptable data rates when investigating particles smaller than 0.1 μm in diameter.

In the case of hot cathode sources a system with two or three electromagnetic condensing lenses is required to demagnify the source spot at the gun to the final spot size. The presently available field emission electron guns are so designed that the extraction and accelerating anode combination is an electrostatic lens capable of producing a focussed electron beam directly at the specimen surface. In this instance, only the use of an aperture beneath the anodes is required to achieve a 250 Å spot size. Scanning coils are added to the electron optical

system to allow the electron probe to be moved about on the specimen as desired. An electromagnetic lens may be added to achieve finer spot sizes.

Visual Displays

The interaction of the electron probe with a specimen generates a number of emissions. These include primary backscattered electrons, secondary backscattered electrons, x-rays, and Auger electrons. Furthermore, if the specimen is sufficiently thin, a portion of the primary beam is transmitted through it as well. The secondary electrons, transmitted electrons, or the primary backscattered electrons can be used to produce visual information. This is done by scanning the beam in a raster fashion on the specimen (such as in TV) and collecting the secondary electrons or transmitted electrons with a suitable detection system. The detectors produce a signal which is used to modulate the intensity of a cathode ray tube (CRT) as the beam of the CRT is scanned synchronously with the electron probe in the instrument. The varying intensity (due to the modulation) of the electron beam of the CRT produces a visual image of the specimen. If TV scan rates are used, a real time display which facilitates the scanning of the specimen for objects of interest is produced. Increased magnification of the specimen is produced by restricting the area of specimen being swept by the electron probe while the dimensions of the display remain fixed (e.g. 100 μm of specimen displayed in 1 cm = 100× magnification and 1 μm of specimen displayed in 1 cm = 10,000× magnification). The secondary electrons have low energy, so that only those generated near the surface are emitted and detected. Consequently, the video display provides topographical information; contrast in the image is produced by topographical differences (Fig. 1). When the transmitted electron signal is displayed, contrast is produced by differences in transmittance of the electrons only. This signal has proved particularly useful when attempting to image fine particles which lie flat on a smooth substrate. The secondary electron signal difference between that from the substrate and such a particle would be very low. When an electron beam instrument is used in the manner described above to produce visual information, the result is known as scanning electron miscroscopy.

X-Ray Spectrometry and Chemical Information

The high-energy electrons interact with the specimen to excite the characteristic x-rays of its constituent elements and a continuous background or brehmsstrahlung radiation. The detection and analysis of the characteristic radiation can be used to obtain qualitative and quantitative chemical information.

Two x-ray spectrometry techniques are primarily used today in conjunction with focussed electron beam excitation. One of these is the wavelength dispersive focussing crystal spectrometer system. The wavelength dispersive system applies Bragg's Law ($n\lambda = 2d \sin \theta_B$) to the problem of measuring the energy (or wavelengths) of the characteristic emitted radiation. A bent and ground crystal of known spacing is used, and its orientation (θ_B) is varied to produce diffraction at any particular wavelength. In this way, characteristic x-ray lines for the various elements are separated from each other. The diffracted rays are detected by a proportional counter and the pulses produced are fed through the usual spectrometer channel (preamplifier, amplifier, pulse height analyzer, and ratemeter or scaler) and recorded (Fig. 2). The θ_B are measured, and the elements present in the specimen are thus determined. The quantity of pulses produced per unit number of incident electrons is a measure of the weight per cent of an element in the sample when compared with the count production in a sample of the pure element and suitably analyzed by applying standard corrections *(16)* or by comparison with standards of known varying compositions. The most precise quantitative data are produced from fairly large, polished specimens.

The major advantage of this type of spectrometer is the excellent energy resolution (1–3 eV FWHM) of which they are capable. This can allow, for example, the determination of the valence state of a particular element in the specimen *(17,18)*. More important, it is this good energy resolution which allows the ready calculation of precise quantitative data.

One of the disadvantages of these spectrometers is that it is necessary for the

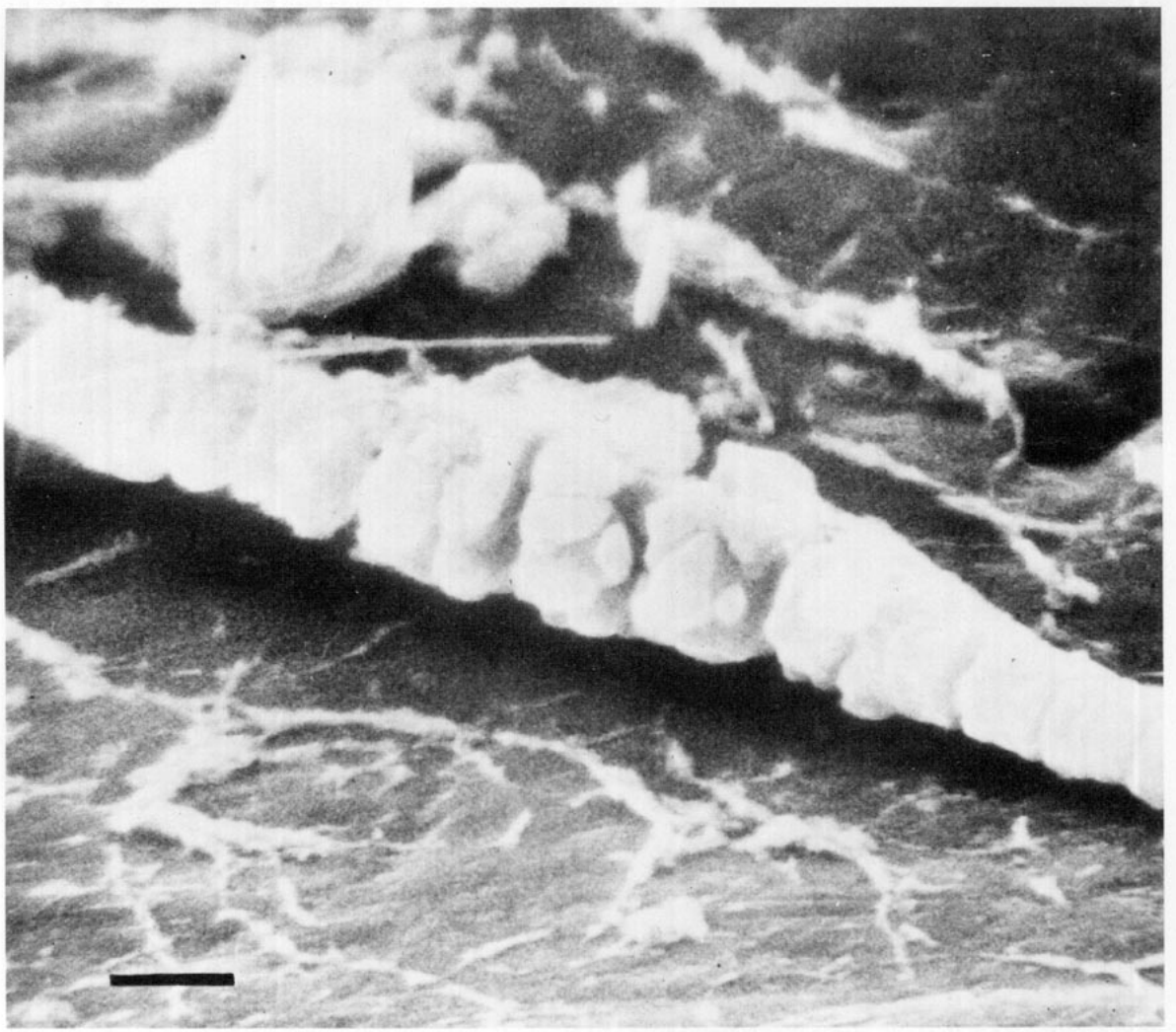

FIGURE 1. Scanning electron micrograph of an asbestos body from the lung of a worker occupationally exposed to amosite asbestos. The image was formed by using the signal from the secondary electron detector. Barmark = 2 μm.

specimen surface to be flat (due to the "focussing" property of the spectrometer in order to obtain reproducible results). Also, these systems are inefficient, requiring high beam currents to produce sufficient x-ray emission to obtain results (thus requiring large probe diameters). Since a spectrometer can detect radiation of only one element at a time, the crystals must be varied through all their orientations to perform a complete qualitative analysis. When done properly, this can be a time-consuming process, on the order of 30 min per spectrum.

The second technique is to use a lithium-drifted silicon crystal with which an incident photon is absorbed and excites a number of electron-hole pairs in the crystal. Each pair production requires an average of 3.6 eV. A bias is applied to the crystal, and the total charge per photon (proportional to the number of pairs produced) is collected and converted to a voltage pulse by a preamplifier. The pulse is further amplified by a linear amplifier producing a final voltage pulse of 0–10 V. This pulse is digitized by an analog-to-digital converter (ADC) and processed by adding a count in a segment of a

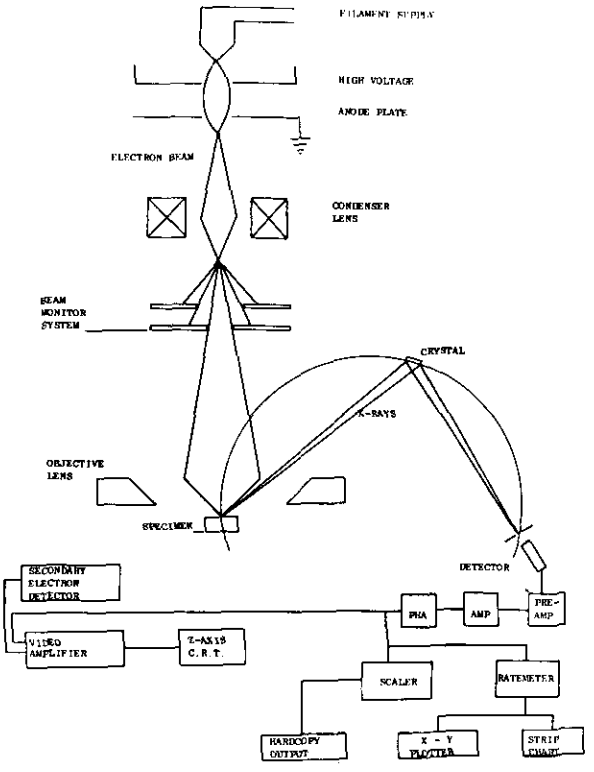

FIGURE 2. Schematic diagram of an electron microprobe with one wavelength dispersive spectrometer shown. Most probes mount at least three such spectrometers. From Langer et al. *(10, 11)*; reprinted with permission.

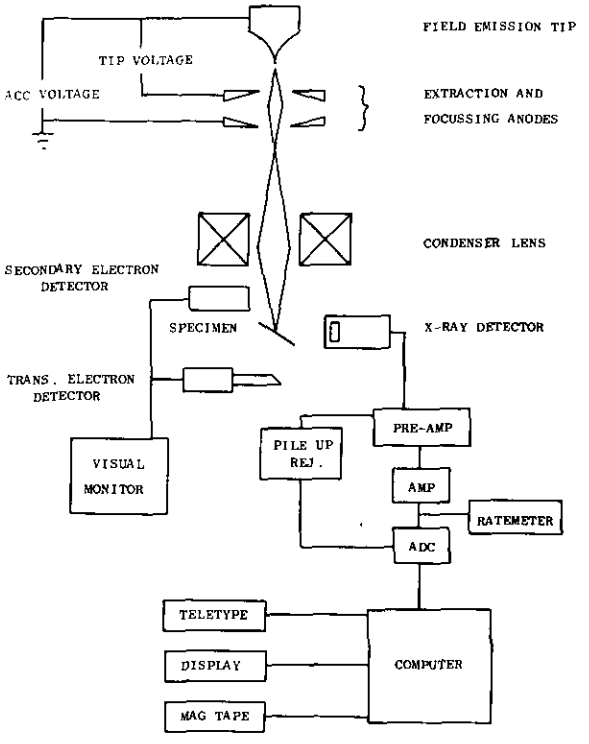

FIGURE 3. Schematic diagram of a scanning electron microscope utilizing a field emission electron source and an energy dispersive x-ray detector.

memory suitably programmed, either in the memory of a hard wired multichannel analyzer or the memory of a computer programmed and interfaced to the ADC (Fig. 3). For example, a 6 keV photon could produce a 6 V pulse at the output of the amplifier which is digitized so that a count is added to segment (called a channel) 600 in the memory.

If the content of the memory is continuously displayed and refreshed, a spectrum containing all lines in the energy region being sampled is observed (Fig. 4). The spectrum can then be recorded on magnetic tape or by some other device.

The energy resolution of this system is about 50 times poorer than a crystal spectrometer (155 eV FWHM at 5.9 keV), not allowing the precision for quantitative calculations or other advantages of high resolution available with geared crystal spectrometers. However, good semiquantitative calculations can be made with

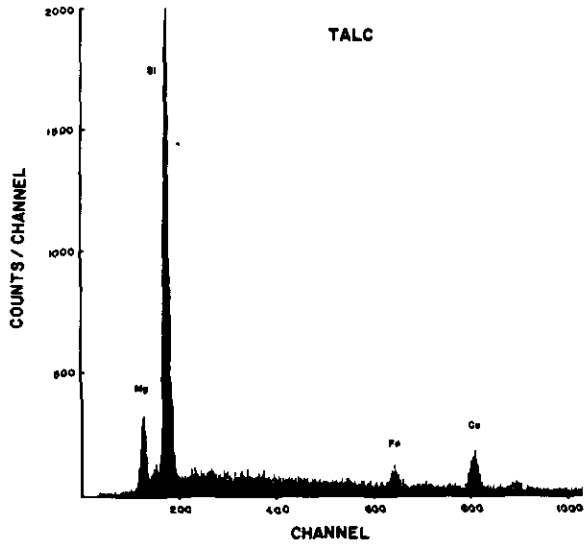

FIGURE 4. Example of a spectrum obtained by energy-dispersive x-ray spectrometry (0–10 keV). The specimen analyzed was a fibrous talc particle. (The copper peak present is due to the specimen support).

proper data handling and the use of good standards. This will be discussed in greater detail below.

There are many advantages to this system, however. The spectrometer detects and processes all photons (0.5–20 keV) in the order in which they are incident at the detector so that essentially all elements are detected concurrently. Thus, complete qualitative data can be acquired about 30 times faster than the wavelength dispersive system (WDS). Furthermore the detector is not as sensitive to variations in specimen height as is the WDS. The third important advantage is the greater efficiency of the system allow the acquisition of data with the much lower currents in the probe at improved spatial resolution conditions, i.e., smaller probe sizes.

Both systems are susceptible to errors which must be accounted for. One problem is that, as the photons generated within the specimen move through it, they can interact with other atoms, causing them to fluoresce and emit their characteristic photons. This is possible if the first photon has an energy in excess of, but near to the absorption edge of, the second atom. The net result is to diminish the apparent intensity of the first element and enhance the intensity of the second. The second problem has a related effect. If the specimen is inclined to the beam and to the detector, the paths the photon must travel are lengthened (or shortened) thereby changing the absorption and fluorescence effects mentioned above.

X-ray spectrometry can be operated in conjunction with scanning optics to provide spatially localized elemental information. While the beam is scanned over the specimen, the signal from a single element can be used to modulate the intensity of the video CRT (instead of the signal from one of the electron detectors used in producing a scanning electron micrograph), and picture points appear where the element under study is present. The result of this operation is to produce a two-dimensional spatial map of the presence of the element in question (Fig. 5).

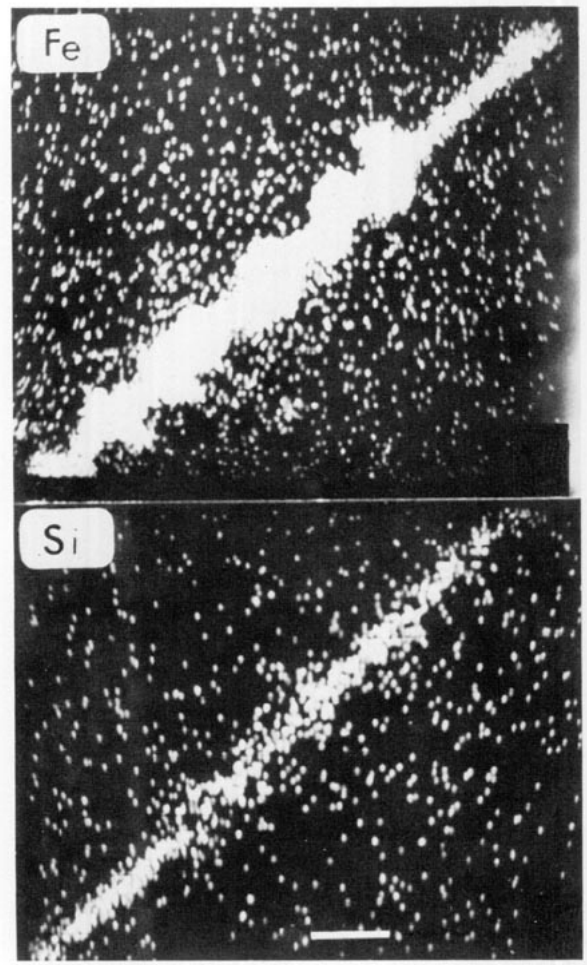

FIGURE 5. Examples of x-ray spatial maps. The specimen was an amosite core asbestos body. The iron rich coating produced the crenulated outline in the Fe map while the Si map shows the straight line placing the fiber at the center of the body. From Langer et al. *(10, 11)*; reprinted with permission. Barmark = 2 μm.

Results of Electron Microprobe Analysis

The first work at this laboratory which applied microchemical analysis to the asbestos problem used an electron microprobe analyzer to investigage asbestos body cores. At the time, the nature of the core was considered of great importance, since the bodies observed with optical microscopy were used as a measure of asbestos exposure, and in general population specimens there was uncertainty as to the nature of the source of the core *(19, 20)*. Microchemical analysis, for reasons given above, was considered the method which would allow differentiation of asbestos type as well as information as to whether or not the core was asbestos.

An asbestos body has an iron-rich coating

which interferes with the analysis, and only bodies with large regions of uncoated fiber were analyzable. In specimens drawn from the general population, too few bodies could be readily found which met this criterion. Furthermore, attempts artificially to expose regions of fibers were not very successful. The conclusion, after much study and work, was reached that it would not be feasible to routinely analyze the cores of asbestos bodies from the general population. The results and details of the work done at this and other laboratories are discussed fully elsewhere *(10, 21, 22)*.

It did appear that it would be useful to apply the technique to uncoated fibers in tissue specimens. This was done with specimens obtained from individuals with occupational exposures to single fiber types (crocidolite, amosite or anthophyllite). The chemical analysis results indicated some magnesium leaching *in vivo* from fiber types with significant magnesium content (anthophyllite, amosite) *(11)*.

After microprobe analysis the area surrounding fibers for which chemical data were obtained was inspected with conventional transmission electron microscopy. It was found that many small fibers were also present, but had been undetected with the standard imaging system of the electron microprobe. This indicated the very real practical limitation that poor spatial resolution presented with respect to asbestos analysis problems and, obviously, to other particulate pollution problems as well.

Applications of Scanning Electron Microscopy X-Ray Analysis

The solution to the problem of analysis of unobserved small particles is the better spatial resolution obtainable with a scanning electron microscope equipped with a compatible x-ray detection system.

The use of the microscope in the transmission mode enhances contrast for small particles (<0.1 μm), eliminates the need for a heavy metal coating and its consequent x-ray interferences and reduces the x-ray background from the substrate which is a thin carbon film. This is particularly significant when smaller particles are analyzed. Further utility is provided because the specimens are compatible with standard transmission microscopy and electron diffraction techniques. The Si(Li) x-ray detector is used to provide maximum data retrieval rates and sufficient semiquantitative chemical information to classify the particles. The SEM x-ray detector combination has been optimized to acquire x-ray spectra from small particles *(23)*. The resulting system is capable of acquiring an x-ray spectrum from particles less than 0.05 μm in diameter in approximately 10^2 sec. Data acquisition times are proportionately faster for larger particles, typically 20 sec for a particle >0.5 μm in diameter. For these large particles, the data acquisition time is determined by the count rate capability of the amplifier for the x-ray detector. The maximum useable output count rate to the multichannel analyzer is approximately 7×10^3 counts/sec.

The x-ray spectrum from each particle is accumulated in the memory of a small computer. After acquisition, the spectrum is stored on magnetic tape with additional alphanumeric information describing the size and shape of the particle. The spectra are then transferred to a larger computer for parameterization, i.e., determination of which elements are present and their relative amounts.

Spectrum parameterization is performed by fitting the content of peaks in the unknown spectrum with the peak content of known single element standards. Following the original work of F. Schamber (Northern Scientific, Middleton, Wisconsin, personal communication), the computer program utilizes a digital spectrum-filtering technique and fits the regions of interest by the least-squares criterion. Figure 6 shows the original x-ray spectrum from tremolite and the spectrum after use of digital filtering. A square search function of zero measure is used. The width of the search function is varied across the spectrum to maintain optimal sensitivity. The result is effectively an averaged second derivative of the original spectrum with the consequent elimination of the linear components of the spectrum. The same procedure is applied to the x-ray spectra obtained from single element standards for each element present in the unknown spectrum to be parameterized.

The least-squares criterion is then used to fit the appropriate linear combination of filtered reference spectra to the filtered unknown spectrum. In this procedure, no attempt is made to

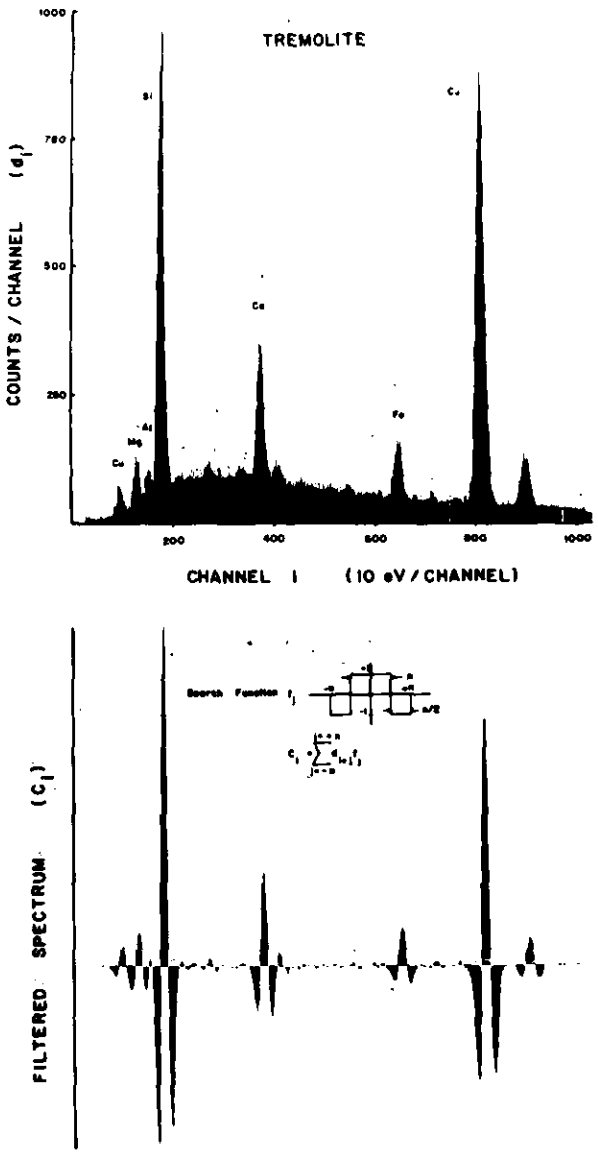

FIGURE 6. Example of raw data spectrum (from a tremolite asbestos fiber) and its associated digitally filtered $(c_i = \sum_{j=-n}^{+n} d_{i+j} f_j)$ spectrum. Note that the background goes to zero in the filtered spectrum. (The copper lines are due to the specimen support).

fit the linear component of the background, since it is first filtered out. Also, no assumptions are made regarding the peak shapes, such as Gaussian, Gaussian with a linear tail, or Gaussian with an exponential tail. The actual peak shapes accumulated in the multichannel analyzer from single element standards are used. The technique also accounts correctly for escape peaks in the spectrum, since they would also be present in spectra from the standards in the same ratios as in the unknown. The problem of unresolved and overlapping peaks is handled satisfactorily by the above procedure, because the positions and shapes of the contaminating peaks are known *(24)*. The program does not make absorption or fluorescence corrections to yield precise quantitative information because the specimens are not uniform polished semi-infinite samples of known orientation. It may be possible to make such corrections by using Monte Carlo calculations, but it has not been found necessary to do so for purposes of classification. Typical examples of spectra from various asbestos types are shown in Figures 6 and 7.

The length of the time required to accumulate an x-ray spectrum suitable for classification is determined by the statistical uncertainty that can be tolerated in the least significant peak. For example, differences between amosite and crocidolite include the magnesium content of the spectrum and the relatively small sodium peak present in the spectrum of crocidolite. Unfortunately, the sodium x-rays are of such low energy that most (75%) are absorbed in the 0.3-mil beryllium window and the surface dead layer of the detector. The result is that one must count for a longer period of time to determine whether or not sodium is present in the spectrum, and at what level. Figure 8 shows the filtered low-energy regions of the spectra of crocidolite and amosite, illustrating the presence of a statistically significant sodium peak in the first and its absence in the latter. Since in pulse counting statistics the standard deviation is equal to the square root of the number of counts, it is necessary to increase counting times by a factor of four to improve the statistics by a factor of two.

The ratios of the elements present in the spectrum are the raw data. The classification (using probe type instrumentation alone) of the particle as to mineral type is based on its size, shape, and chemical composition. The representation of the chemical composition and the classification of the particle as to type is relatively straightforward if the total number of detect-

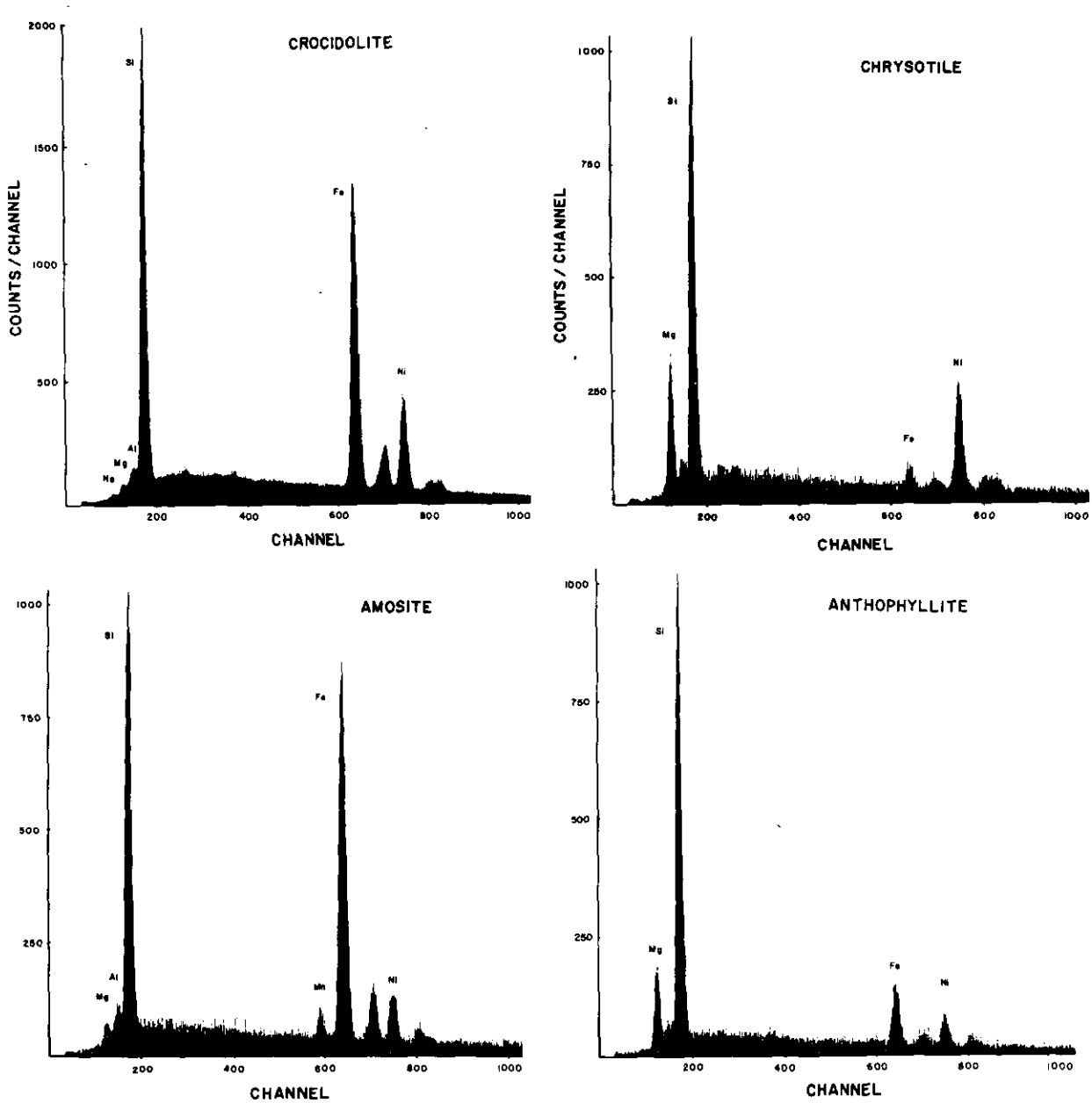

FIGURE 7. Examples of typical spectra from different types of asbestos: amosite; crocidolite; chrysotile; anthophyllite. (The nickel lines are present due to the specimen support.)

able elements is three or less. The three-component diagram with the convention that the sum of the components equals unity is conveniently used. It is possible to represent a four-component system on a ternary diagram by using different symbols to distinguish the fourth component with respect to a preset level. Another alternative is to use a single apex to represent the sum of two or more elements where mineralogically appropriate. The resulting plots of pseudo-composition will show a range of composition corresponding to the varying composition of the original mineral. There is also the variation in the parameterized composition due to the statistical uncertainty of the original measurement and the fact that no

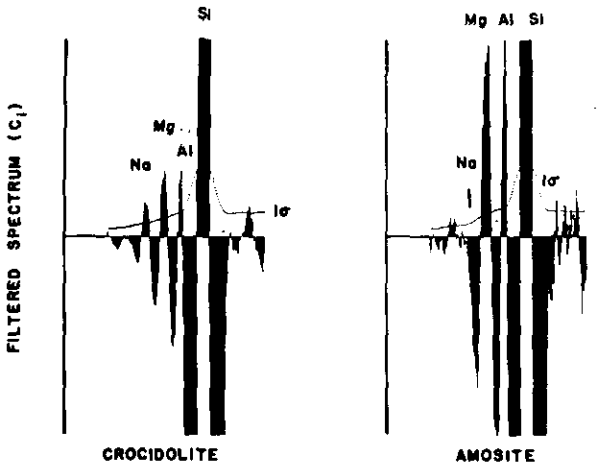

FIGURE 8. Result of digitally filtering the spectra for amosite and crocidolite showing the low energy region (0–2 keV). The presence of sodium is shown to be statistically significant in the spectrum from crocidolite but is not present in that of amosite.

fluorescence and absorption corrections are made. A typical example of the use of the three-component diagrams for the characterization and identification of asbestos types is shown in Figure 9. The clustering of the analyses and the range of compositions are indicated on the plot.

Three-component diagrams have proved to be very useful, but within clearly defined limits. The first limitation is the case of fibrous particles with similar chemistries. A good example

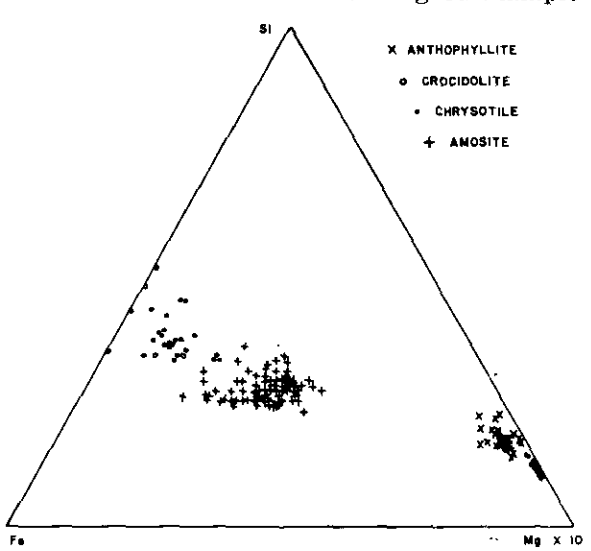

FIGURE 9. Three-component diagram with analyses of four kinds of asbestos minerals plotted.

is the attempt to separate the minerals chrysotile, anthophyllite, and fibrous talc, The elemental compositions are quite similar, but the crystal structures are different. It is relatively simple to distinguish them on the basis of morphology and electron diffraction, but more difficult on the basis of elemental composition alone. Figure 10 shows a Mg–Si–Fe three-component diagram for the three minerals. This points out the necessity of using all available information and techniques, such as conventional transmission electron microscopy and selected-area electron diffraction, in cases where classification is ambiguous.

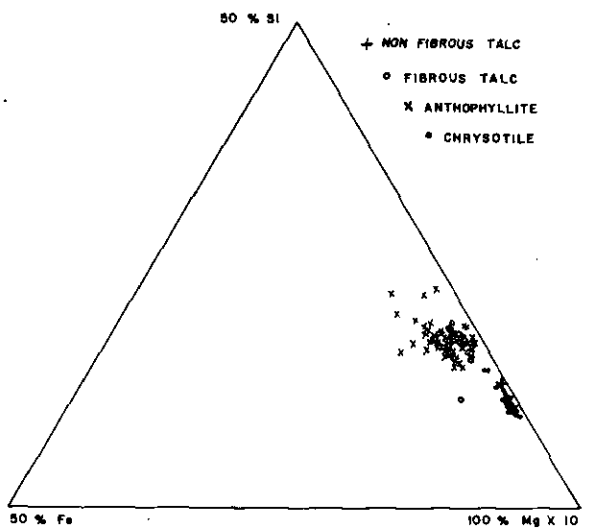

FIGURE 10. Plot of three-component analyses of anthophyllite, chrysotile, and fibrous talc illustrating the insufficiency of the probe technique to allow certain differentiation.

The case of known asbestos types in a background of completely unknown particles is another in which the use of three-component diagrams is limited. The problem is that only three parameters are represented on the diagram, while there may be unknown particles that are fibrous which contain additional elements distinguishing them from asbestos but whose three-component ratios plot the same as a known asbestos type. All of the available information useful for classification is not represented on the three-component diagram.

The inability to measure quantitatively the probability of a correct classification is another limitation of three-component diagrams. The

classification of a particle requires the operator to make an individual judgment for every particle. This is not a serious limitation when the nature of the sample is known and the distinction is obvious. For example, Table 1 lists the nominal range of composition for the various asbestos minerals and some of the other particulates from which it may be necessary to distinguish them in a particular sample. If a sample contains only anthophyllite and tremolite, for example, the operator would have no difficulty distinguishing them with negligible probability of error. A mixture of anthophyllite and chrysotile would present problems because of the compositional overlap mentioned before. It would be of value to have a measure of the probability of a correct classification in such cases.

The final limitation of the three-component diagrams is the inability to utilize the size and shape information in a formalized way. The SEM-microprobe technique cannot be fully exploited without a more generalized scheme for particle characterization. This becomes even more evident when one realizes that in all the problems discussed above, prior knowledge of the particles of interest was available. If a problem such as particulate pollution of urban air is considered, the need for a general classification scheme, where no single group of particles is of interest *a priori*, becomes more obvious.

Some work on the automatic classification of particles has been applied to the coal dust problem. This was done utilizing preselected channels of information *(25, 26)*. Among the possible generalized procedures that we have considered for classifying particles according to elemental composition, size and shape, two appear to be most promising. The first possibility involves the use of a decision tree with the application of a discriminant function at each node of the tree. Figure 11 illustrates how such a procedure might be used to classify the various asbestos types in a matrix of talc and clay.

At each node of the tree, a function F of all of the available parameters, X_i is calculated to maximize the difference between the two subclasses of particles. For example, at the node distinguishing two classes of particles, the result of calculating $F\ (X_1,\ X_2, \ldots X_n)$ for each particle in the mixture might be as shown in Figure 12. Where the analyses overlap, no positive classification is possible. The decision tree presented here is schematic and should be considered only a possible framework for approaching the classification of the asbestos minerals and the information required for a correct classification. As stated before, the greatest ambiguity in such a scheme would be in the

Table 1. Chemical composition of common fibrous silicate minerals.

	Typical ranges, wt-%								
	SiO_2	MgO	FeO	Fe_2O_3	Al_2O_3	CaO	K_2O	Na_2O	H_2O
Chrysotile	38–44	40–43	0–0.8	0.5–4	0.3–0.9	0–1.0	Trace	Trace	13–14
Crocidolite	49–53	0–3	13–20	17–20	0–0.2	0.3–2.7	0–0.4	4–8.5	2.5–4.5
Amosite	49–53	1–7	34–44	—	—	—	0–0.4	Trace	2.5–4.5
Anthophyllite	56–58	28–34	3–12	—	0.5–1.5	—	—	—	1–6
Actinolite	51–56	15–20	5–15	0–3	1.5–3	10–12	0–0.5	0.5–1.5	1.5–2.5
Tremolite	55–60	21–26	0–4	0–0.5	0–2.5	11–13	0–0.6	0–1.5	0.5–2.5
Talc	60–63	30–32	0.6–2.5	0–1.5	0–2.5	0–1.4	—	—	0–0.3
Hornblende	39–54	3–25	0.2–23	0–9	4–15	9–13	0–1.7	0.5–4.3	0–2.6
Orthopyroxene	44–60	4–39	3.5–48	0–3	0–8	0.2–4.2	0–0.6	0–0.9	0–0.8

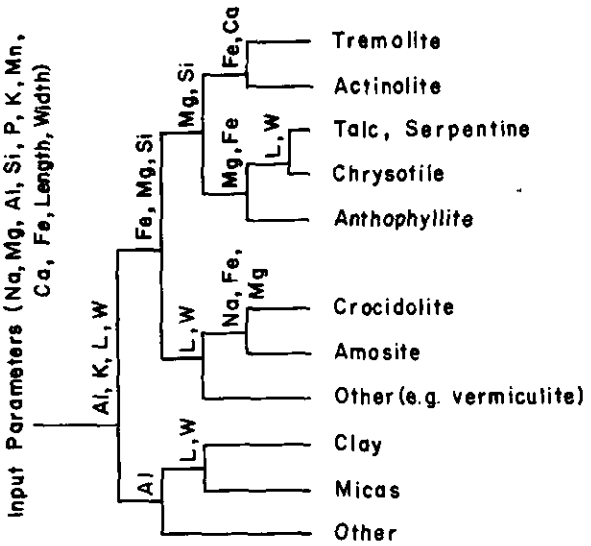

FIGURE 11. Possible discriminant tree to be used for distinguishing a number of different minerals with only electron probe data as its input parameters.

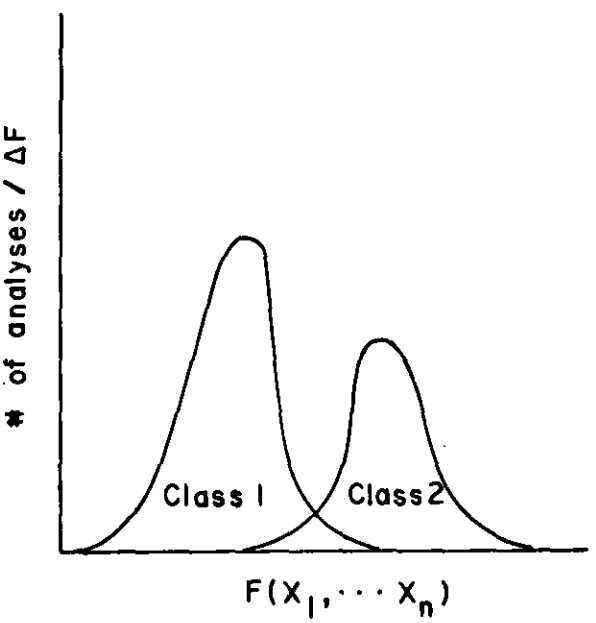

FIGURE 12. Schematic representation of the result of calculating the discriminant function at a node of the decision tree in Figure 11.

separation of talc, chrysotile, and other serpentine minerals. It is important that all available mineralogical information about the specimen be used to help in the identification process.

A second possible approach to the classification of particles involves the application of multivariate analysis of variances of the parameters determined for each particle. By this procedure all possible pairs of parameters are considered and percentile contours determined for each class of particles. Figure 13 is a schematic representation of the data determined in such a procedure. The classification of each particle would then be based on the calculation of highest probability for inclusion within all the predetermined contours.

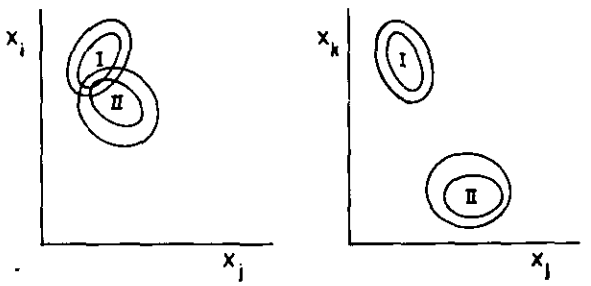

FIGURE 13. Schematic representation of the percentile contour approach to particle classification. The particles are not separable when the parameters X_i and X_j are considered, but they are when X_k and X_j are examined. All possible pairs of parameters would have to be considered.

Both of the possible classification procedures outlined above require that suitable "pure" mineral standards be available for analysis before the unknown sample is examined. This is not an unreasonable requirement if a catalog of all x-ray spectra, or at least the parameterizations of such spectra, can be maintained in a suitable format for later analysis. Both methods outlined above are amenable to automatic classification procedures and the calculation of the probability of a correct classification.

At the present time, the ultimate limits of the SEM microprobe technique described above are not known, in terms of its ability to correctly classify general microparticles. The applicability of the method depends on the particular sample being studied and the fineness of the distinctions which must be made. It is possible, however, to define the limits encountered in the present system which has been optimized for such small particle work. The first limitation consists of the fact that no crystallographic in-

formation about the particle is obtained; therefore, if a sample consists of particles of the same size and shape with similar composition and differing only in crystallographic form, no accurate classification can be made on the basis of microprobe analysis alone. A second limitation is that imposed by the Si(Li) x-ray detector and its inability to detect routinely elements lighter than sodium. A sample of iron oxide and iron nitride spheroids could not be distinguished on the basis of their associated spectra. The third limitation is that of contamination of the x-ray spectrum of the particle of interest by x-rays generated in particles nearby *(23)*. This problem can be alleviated by having a suitably dispersed sample. The final limitations are those imposed by the nature of the process of x-ray generation and detection. If a time constraint of 10^2 sec is imposed for the acquisition of the x-ray spectrum, our work would indicate a lower limit of detectability for silicate particles in the range of 0.05 μm in diameter.

Conclusion

The electron microanalytical technique has been shown to have excellent utility with respect to the problem of identifying and differentiating asbestos fibers in air, water and tissue specimens. A wide range of mixtures can be examined fruitfully with data analysis techniques presently available. These include distinguishing asbestos types in a mixture known to contain only asbestos, distinguishing an asbestos type in a mixture where the other major components are known, and isolating asbestos where other unknown minerals are present. Conventional electron microscopy and selected area electron diffraction may be necessary to make final determinations, but this depends on the population of particle types present.

Ultimately, the techniques discussed herein can be applied to particulate mixes where no single particle type is of interest *a priori*. Such a sample might be drawn from the ambient urban atmosphere where it is desired to classify the major component populations. Such studies could be best accomplished by automated instrumentation, and classification schemes described above could be applied and would be the critical step.

Acknowledgments

We wish to thank Fred Schamber of Northern Scientific Inc. whose original work on the parameterization of multichannel analyzer data was followed closely, and Sun Yu of the Computer Sciences Department, Mount Sinai School of Medicine, for help in the programming of the data analysis algorithms. Thanks are also due to Dr. A. M. Langer and Dr. A. Rohl of the Environmental Sciences Laboratory, Sinai School of Medicine, for their many helpful discussions concerning the chemistry and crystallography of asbestos and related minerals. This work was supported by NIEHS grants ES–00752 and ES–00928.

REFERENCES

1. Selikoff, I. J., Churg, J., and Hammond, E. C. Asbestos exposure and neoplasia. JAMA **188:** 22 (1964).
2. Selikoff, I. J., Hammond, E. C., and Churg, J. Carcinogenicity of amosite asbestos. Arch. Environ. Health **25:** 183 (1972).
3. Wagner, J. C., Sleggs, C. A., and Marchand, P. Diffuse pleural mesothelioma and asbestos exposure in the North Western Cape Province, Brit. J. Ind. Med. **17:** 260 (1960).
4. Speil, S., and Leinweber, J. P. Asbestos minerals in modern technology. Environ. Res. **2:** 166 (1969).
5. Yada, K. Study of chrysotile asbestos by a high resolution electron microscope. Acta Cryst. **23:** 704 (1967).
6. Langer, A. M., Mackler, A., and Pooley, F. D. Electron microscopical investigation of asbestos fibers. Environ. Health Perspect. **9:** 63 (1974).
7. Maggiore, C. J. Automated asbestos analysis. Final report, EPA Contract CPA 70–92 (1971).
8. Timbrell, V., Pooley, F., and Wagner, J. C. Characteristics of respirable asbestos fibres. In: Pneumoconiosis, Proceedings International Conference Johannesburg, 1969. H.A. Shapiro, Ed., Oxford Univ. Press-Capetown, 1970, p.120.
9. Skikne, M. I., Talbot, J. H., and Rendall, R. E. G. Electron diffraction patterns of U.I.C.C. asbestos samples. Environ. Res. **4:** 141 (1971).
10. Langer, A. M., Rubin, I. B., and Selikoff, I. J. Chemical characterization of asbestos body cores by electron microprobe analysis. J. Histochem. Cytochem. **20:** 723 (1972).
11. Langer, A. M., et al. Chemical characterization of uncoated asbestos fibers from the lungs of asbestos workers by electron microprobe analysis. J. Histochem. Cytochem. **20:** 735. (1972).
12. Crewe, A. V., et al. Electron gun using a field emission source. Rev. Sci. Instr. **39:** 576 (1968).
13. Crewe, A. V., Wall, J., and Welter, L. M. A high resolution scanning transmission electron microscope. J. Appl. Phys. **39:** 5861 (1968).

14. Broers, A. N., and Brandes, E. K. High resolution reflection scanning electron microscopy. In: Scanning Electron Microscopy/1969: Proceedings of the Second Annual Scanning Electron Microscope Symposium. O. Johari, Ed., Illinois Inst. Technol. Research Institute, Chicago, 1973, p. 15.
15. Ahmed, H., and Nixon, W.C. Boride guns for high level scanning electron microscopy. In: Scanning Electron Microscopy/1973: Proceedings of the Sixth Annual Scanning Electron Microscope Symposium. O. Johari, Ed. Illinois Institute of Technology Research Institute, Chicago, 1973, p. 217.
16. Quantitative electron probe microanalysis. K.F.J. Heinrich, Ed. National Bureau of Standards. SP 298 1968.
17. Baun, W. L., and Fischer, D. W. The effect of valence and coordination on K series diagram and nondiagram lines of Mg, Al, and Si. Advan. X-Ray Anal. **8:** 371. (1965).
18. Landstrom, D. K., and Kohler, D. Electron microprobe analysis of atmospheric aerosols. NAPCA Final Report (Contract CPA 22-69-33) 1969; NITS PB 189 282.
19. Cooke, W. E. Asbestos dust and curious bodies found in pulmonary asbestosis. Brit. Med. J. **2:** 578 (1929).
20. Williams, E. "Curious bodies" found in the lungs of coal workers. Lancet **2:** 541 (1933).
21. Stumphius, J., and Meyer, P. B. Asbestos bodies and mesothelioma. Ann. Occup. Hyg. **11:** 283. (1968).
22. Andersen, C. A. An introduction to the electron probe microanalyzer and its application to biochemistry. In: Methods of Biochemical Analysis, Vol. 15, D. Glick, Ed., Interscience, New York, 1967, p. 147.
23. Maggiore, C. J., and Rubin, I. B. Optimization of an SEM x-ray spectrometer system for the identification and characterization of ultramicroscopic particles. In: Scanning Electron Microscopy/1973: Proceedings of the Sixth Annual Scanning Electron Microscope Symposium, O. Johari, Ed., Illinois Inst. Technol. Research Institute, Chicago, 1973 p. 129.
24. Trombka, J. I. Analysis of x-ray pulse height spectra. Ph.D. thesis, Univ. Michigan, Ann Arbor; Dissert. Abstr. **23:** 193 (1962).
25. White, E. W., and DeNee, P. B. Characterization of coal mine dust by computer processing of scanning electron microscope information. In: Coal Workers Pneumoconiosis. I. J. Selikoff, M. M. Key, and D. H. K. Lee, Eds., N.Y. Academy of Sciences, New York 1972.
26. Lebiedzik, J., et al. New methods for quantitative characterization of multiphase particulate materials including thickness measurements. In: Scanning Microscopy/1973: Proceedings of the Sixth Annual Scanning Electron Microscope Symposium, O. Johari, Ed., Illinois Inst. Technol. Research Institute, Chicago, 1973, p. 122.